Emergence of ferromagnetism in antiferromagnetic $TbMnO_3$ by epitaxial strain

X. Marti,[1,a)] V. Skumryev,[2] C. Ferrater,[3] M. V. García-Cuenca,[3] M. Varela,[3] F. Sánchez,[1] and J. Fontcuberta[1]
[1]*Institut de Ciència de Materials de Barcelona (ICMAB-CSIC), Campus UAB, 08193 Bellaterra, Spain*
[2]*Departament de Física, Universitat Autònoma de Barcelona, 08193 Bellaterra, Spain and Institució Catalana de Recerca i Estudis Avançats (ICREA), 08010 Barcelona, Spain*
[3]*FAO and IN2UB, Universitat de Barcelona, Martí i Franquès 1, 08028 Barcelona, Spain*

(Received 27 March 2010; accepted 13 May 2010; published online 2 June 2010)

We show that in oxide thin films of spiral antiferromagnetic orthorhombic $TbMnO_3$, ferromagnetism emerges resulting from epitaxially induced strain. The unit cell volume can be tuned (contracting up to a 2%) by varying thickness and deposition conditions; it is found that the ferromagnetic response correlates with the unit cell deformation. Such effect of strain on the magnetic properties turns out to be similar to that occurring in collinear orthorhombic antiferromagnets such as $YMnO_3$. Owing to the intimate relationship between magnetic order and ferroelectricity in $TbMnO_3$ these results may provide a new route to induce magnetoelectric coupling and tailor their ferroelectric response.
 [doi:10.1063/1.3443714]

The coupling of ferroelectricity and ferromagnetism in a single material or heterostructure attracts much attention due to its promising applications in sensor and data storage technologies. The scarcity of materials which individually display this feature[1] triggered the development of varied strategies where, for instance, the coupling is mediated by elastic[2] or exchange-bias[3] effects. Particularly relevant is the discovery that ferroelectricity can be obtained subsequent to magnetic ordering. Antiferromagnetic orthorhombic rare earth manganites ($RMnO_3$) probably constitute the best known example of such materials. Either if the magnetic structure is collinear (E-type as in $YMnO_3$ (YMO) (Ref. 4) or ($HoMnO_3$) (Ref. 5) or noncollinear [spiral as in $TbMnO_3$ (TMO)],[6] magnetic interactions give rise to atomic displacements destroying the center of symmetry and thus allowing an electrical polarization.[7] Due to this intimate link between magnetic structure and ferroelectricity, changes in the electrical polarization upon applied magnetic fields are to be expected. Indeed, it was the early experimental observation of such effects in bulk TMO (Ref. 8) that triggered intensive theoretical research and exploration of epitaxial thin films. However, investigation of magnetic properties on $RMnO_3$ films (Refs. 9–17) revealed the unexpected existence of a ferromagnetic response in otherwise bulk antiferromagnetic materials. Whereas in the case of E-type spin-ordered structures, its origin has been attributed to strain-induced deformation of the unit cell and subsequent unbalancing of magnetic interactions,[9–12,17] it also has been proposed domain walls boundaries to be relevant in the case of the spiral $TbMnO_3$.[16] However, it turns out that the signatures of ferromagnetism reported[9–17] are in all cases intriguingly similar. Whether the origin of the ferromagnetism in both compounds is the same irrespective of their bulk magnetic structure is a critical open issue that we aim to disentangle in this paper.

We report here on the magnetic properties of epitaxial TMO thin films. Data shows that the ferromagnetic response can be selected at wish by tuning the unit cell volume (V_C) through the film thickness and deposition conditions. Of relevance here is that the obtained V_C versus ferromagnetism correlation clearly resembles that reported for orthorhombic YMO thin films indicating that its origin does not depend on the bulk magnetic structure and it is strongly related to the unit cell distortion.

Thin films were deposited by pulsed laser deposition using a KrF excimer laser focused on a stoichiometric $TbMnO_3$ target with the fluence and the repetition rate set to 1.5 J/cm^2 and 5 Hz, respectively. Films were grown on (001)-oriented $SrTiO_3$ (STO) substrates, heated at 785 °C and placed at 5 cm from the target. A set of samples were grown at 0.1, 0.2, 0.3, and 0.4 mbar oxygen pressure; the laser pulses were adjusted to obtain films with thickness around 40 nm. This set of samples was completed with three thicker films grown at fixed pressure (0.3 mbar) and being 95, 137, and 140 nm thick. Crystal structure was investigated using four-circle x-ray diffractometer. Magnetic data were recorded using a superconducting quantum interference device with the magnetic field applied parallel to the sample surface.

Figure 1(a) shows the $\theta/2\theta$ scan of a selected TMO sample (38 nm thick, 0.3 mbar). Only reflections corresponding to the substrate and to the TMO(001) planes are observed indicating that the films are c-textured note the *Pbnm* settings is used.[18] φ-scans around the (111) reflections of the substrate and the film are shown in Fig. 1(b). Four narrow substrate STO(111) peaks, 90° in-plane spaced, are visible in Fig. 1(b), together with four o-TMO(111) reflections, located at 45° from each STO(111) reflection; this indicates that the in-plane axes (a, b) of the film are 45° in-plane rotated respect to the [100] direction of the substrate. The broadening of the TMO(111) peaks results from the existence of 90° in-plane twinning, as we have exhaustively analyzed for o-YMO(001)/STO(001) films.[19] Reciprocal space maps around the TMO(208) and TMO(028) reflections are shown in Figs. 1(c) and 1(d), respectively. The crossing of the dashed lines in these plots signals the location for the corre-

a)Electronic mail: xavi.mr@gmail.com.

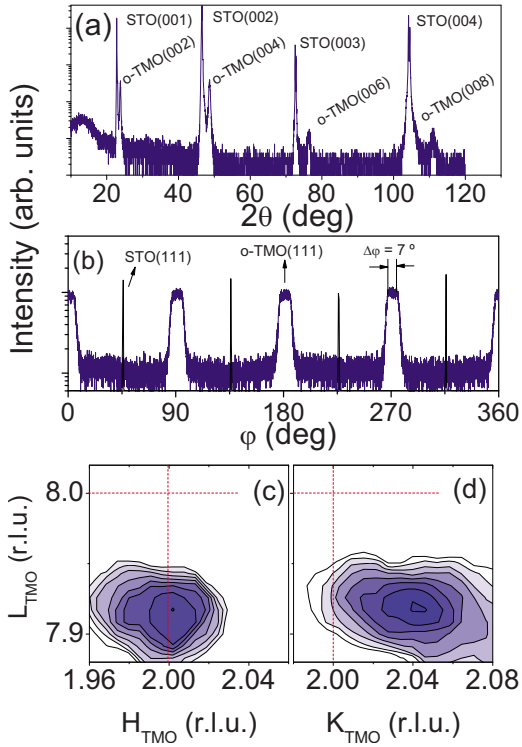

FIG. 1. (Color online) (a) $\theta/2\theta$ scans for a selected TMO (38 nm, 0.3 mbar) sample indicating (001) texture with no traces of other contributions. (b) φ-scan around the STO(111) and TMO(111) reflections evidencing the epitaxial order in o-TMO films. Reciprocal space maps around the (c) TMO(208) and (d) TMO(028) reflections.

sponding bulk TMO reflections. Figure 1(c) shows that the in-plane component of the (208) reflection is observed exactly at the bulk position thus implying that the *a* parameter is fully relaxed. In contrast, data in Fig. 1(d) show that the (028) reflection is shifted toward larger K values indicating that *b* parameter is compressively strained. On the other hand, the *c* parameter is elongated as evidenced in both plots by the shorter L of the corresponding reflections. It turns out that, similarity to what was observed in o-YMO films,[11,18] epitaxial strain is anisotropic being zero, tensile, and compressive along the [100], [001], and [010] directions, respectively. These observations are common to all TMO samples produced. As a consequence of these distortions, the unit cell volume can be contracted up to 2%.

We now turn to the magnetic characterization of the films. Figure 2 shows the inverse susceptibility $\chi^{-1}(T)$ of the thickest TMO sample available (140 nm) measured after field cooled (FC) at two different magnetic fields (10 and 20 kOe) applied in the plane of the film. We focus our attention to the high temperature paramagnetic regime, $T \gg 40$ K. We note that susceptibility values measured at different fields coincide thus indicating the absence of spurious ferromagnetic contributions.[20] The extrapolation of the linear regime of susceptibility curves to lower temperatures reveals that the intersection with the horizontal axis is around $\theta_p = 0$ in agreement with previous data on bulk TMO (Ref. 21) measured along the b-axis. In agreement with bulk measurements, the absence of a well-defined antiferromagnetic up-turn at $\chi^{-1}(T_N)$, visible in YMO films,[11] indicates that the paramagnetic susceptibility is dominated by Tb^{3+} ions.[22] The slope of the inverse susceptibility versus temperature leads to a Curie constant $C \approx 7.22$ K which corresponds to and effective

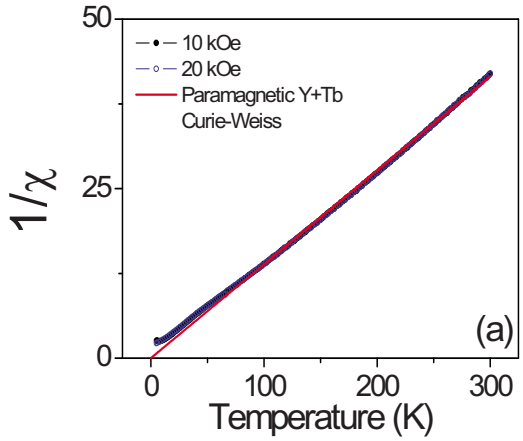

FIG. 2. (Color online) Inverse susceptibility $1/\chi$ measured at different magnetic fields for a selected TMO sample (140 nm thick, 0.3 mbar).

magnetic moment $\mu_{eff} \approx 12(2)\ \mu_B$ which is in agreement with that expected $\{\mu_{eff} = \sqrt{[\mu^2_{eff}(Tb) + \mu^2_{eff}(Mn)]} = 11\ \mu_B\}$ for the contribution from Tb^{3+} and Mn^{3+} ions $[\mu_{eff}(Tb) = 9.72\ \mu_B$ and $\mu_{eff}(Mn) = 4.90\ \mu_B]$.

Figures 3(a)–3(c) show the zero-field cooled (ZFC) and the FC (ZFC-FC) magnetization curves of few representative samples having distinct V_C values. A clear splitting of both curves is well visible revealing a net magnetization. The splitting emerges intriguingly close to the bulk antiferromagnetic ordering ($T_N \sim 40$ K) and at slightly increasing temperatures as the unit cell volume contracts. It suggests that the ferromagnetic ordering is closely related to the pristine antiferromagnetic ordering and, at the same time, it depends on the unit cell distortion. Indeed, data shows that the ZFC-FC splitting increases when shrinking V_C. Identical be-

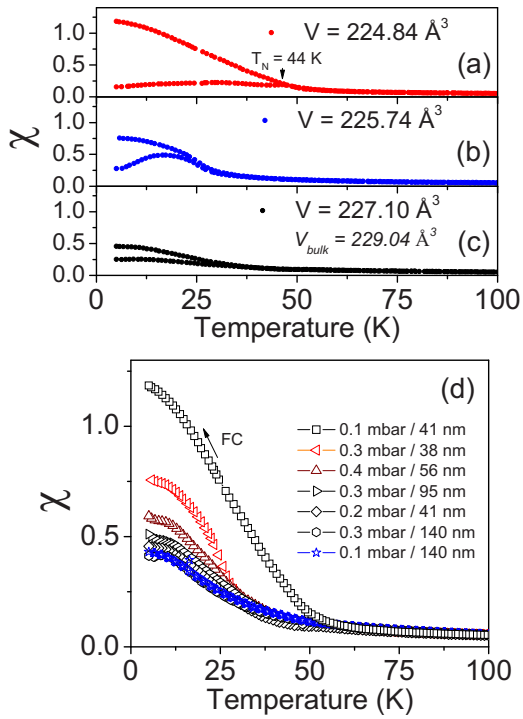

FIG. 3. (Color online) ZFC-FC curves for three TMO samples of the labeled unit cell volume are shown in panels (a)–(c). Samples were grown at 0.1 mbar, 0.2 mbar, and 0.3 mbar with thicknesses 41 nm, 41 nm, and 38 nm, respectively. (d) FC curves for the complete set of samples. All measurements have been performed at 500 Oe applied in-plane of the sample.

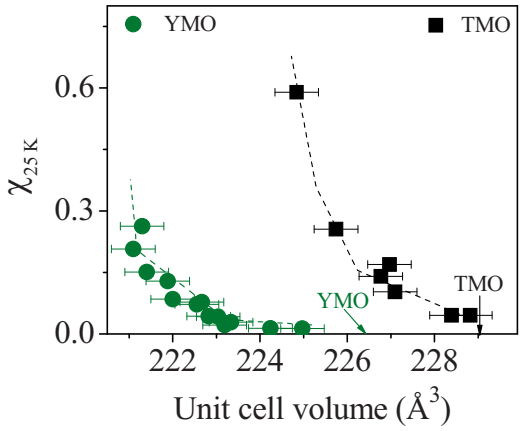

FIG. 4. (Color online) Susceptibility at 25 K vs unit cell volume for YMO and TMO thin films. Both compounds display the same trend despite the different bulk magnetic ground structure. Arrows signal the bulk unit cell volumes.

havior is found in all films as shown in Fig. 3(d), where only FC curves are included for the sake of clarity. Note that data clearly resembles the behavior reported for YMO films[11] and Y^{3+} is a nonmagnetic atom. Owing to this similarity and the fact that the net magnetic moment is observed well above the expected Tb^{3+} ions ferromagnetic ordering, it turns out plausible that the ZFC-FC splitting is caused only by the Mn sublattice.

Following the criteria we already used for YMO films,[11] we plot in Fig. 4 the dependence of χ(T=25 K) on V_C aiming to quantitatively evaluate how epitaxial strain is inducing the weak ferromagnetism. In contrast to our early work on YMO,[11] we used V_c instead of the strain along [010] to correlate the magnetic response because the observed trend is identical but V_c includes all structural distortions. We have subtracted the paramagnetic contribution of Tb^{3+} ions to evaluate the contribution of the magnetically ordered $Mn^{3+}O_3$ sublattice: this allows comparing the strain-induced magnetization to that reported for YMO films in Ref. 11. Data in Fig. 4 collects the main finding here, that is the ferromagnetic response of the TMO films is determined by the unit cell contraction and its behavior mimics that reported for YMO films.[11] It thus follows that the magnetic structure of the pristine bulk material, that is its spiral or collinear orders are not relevant to the magnetic response of strained YMO or TMO films. Indeed, the evident similarity between magnetic properties in strained YMO and TMO films suggest that the magnetic structure could be similar in both strained films thus vanishing the boundary between E-type (YMO) (Ref. 4) and spiral (TMO) (Ref. 6) magnetic orderings existing in bulk orthorhombic rare earth manganites. As suggested in Ref. 16, a possible scenario could be that epitaxial strain primarily suppresses the spiral order in $TbMnO_3$ in favor of the E-type as found in $YMnO_3$. Subsequent strain-unbalanced magnetic interactions may lead to the observed weak ferromagnetic response as found in $YMnO_3$.[11]

In summary, we have shown that by gradually contracting the unit cell of epitaxial TMO(001) thin films a ferromagnetic response gradually emerges. The present work shows that despite the fact that the bulk magnetic ground structure of $TbMnO_3$ is spiral, the changes in the magnetic structure upon epitaxial strain follow the same pattern as observed in the strained YMO films having a collinear (E-type) ground magnetic structure. Therefore, it follows that in $TbMnO_3$ can be made (weak) ferromagnetic under strain. Although it remains to be seen that the ferroelectric character is preserved, recent results[23] on the closely related $YMnO_3$ strongly suggest that strained $TbMnO_3$ films may become a new member of the reduced family of biferroic: ferromagnetic and ferroelectric, materials.

Financial support by the Ministerio de Ciencia e Innovación of the Spanish Government (Project Nos. MAT2008-06761-C03 and NANOSELECT CSD2007-00041) and Generalitat de Catalunya (Grant No. 2009 SGR 00376) is acknowledged.

[1]N. A. Hill, J. Phys. Chem. B **104**, 6694 (2000).
[2]H. Zheng, J. Wang, S. E. Lofland, Z. Ma, L. Mohaddes-Ardabili, T. Zhao, L. Salamanca-Riba, S. R. Shinde, S. B. Ogale, F. Bai, D. Viehland, Y. Jia, D. G. Schlom, M. Wuttig, A. Roytburd, and R. Ramesh, Science **303**, 661 (2004).
[3]V. Laukhin, V. Skumryev, X. Marti, D. Hravobsky, F. Sánchez, M. V. García-Cuenca, C. Ferrater, M. Varela, U. Lüders, J. F. Bobo, and J. Fontcuberta, Phys. Rev. Lett. **97**, 227201 (2006).
[4]A. Muñoz, J. A. Alonso, M. T. Casais, M. J. Martínez-Lope, J. L. Martínez, and M. T. Fernández-Díaz, J. Phys.: Condens. Matter **14**, 3285 (2002).
[5]A. Muñoz, M. T. Casais, J. A. Alonso, M. J. Martínez-Lope, J. L. Martínez, and M. T. Fernández-Díaz, Inorg. Chem. **40**, 1020 (2001).
[6]R. Kajimoto, H. Yoshizawa, H. Shintani, T. Kimura, and Y. Tokura, Phys. Rev. B **70**, 012401 (2004).
[7]See, for instance, D. Khomskii, Phys. **2**, 20 (2009).
[8]T. Kimura, T. Goto, H. Shintani, K. Ishizaka, T. Arima, and Y. Tokura, Nature (London) **426**, 55 (2003).
[9]X. Martí, V. Skumryev, V. Laukhin, F. Sánchez, C. Ferrater, M. V. García-Cuenca, M. Varela, and J. Fontcuberta, J. Mater. Res. **22**, 2096 (2007).
[10]T. H. Lin, H. C. Shih, C. C. Hsieh, C. W. Luo, J.-Y. Lin, J. L. Her, H. D. Yang, C.-H. Hsu, K. H. Wu, T. M. Uen, and J. Y. Juang, J. Phys.: Condens. Matter **21**, 026013 (2009).
[11]X. Marti, V. Skumryev, A. Cattoni, R. Bertacco, V. Laukhin, C. Ferrater, M. V. García-Cuenca, M. Varela, F. Sánchez, and J. Fontcuberta, J. Magn. Magn. Mater. **321**, 1719 (2009).
[12]C. C. Hsieh, T. H. Lin, H. C. Shih, C.-H. Shu, C. W. Luo, L.-Y. Lin, K. H. Wu, T. M. Uen, and J. Y. Juang, J. Appl. Phys. **104**, 103912 (2008).
[13]B.J. Kirby, D. Kan, A. Luykx, M. Murakami, D. Kundaliya, and I. Takeuchi, J. Appl. Phys. **105**, 07D917 (2009).
[14]D. Rubi, S. Venkatesan, B. J. Kooi, J. Th. M. De Hosson, T. T. M. Palstra, and B. Noheda, Phys. Rev. B **78**, 020408 (2008).
[15]D. Rubi, C. de Graaf, C. J. M. Daumont, D. Mannix, R. Broer, and B. Noheda, Phys. Rev. B **79**, 014416 (2009).
[16]C. J. M. Daumont, D. Mannix, S. Venkatessan, G. Catalan, D. Rubi, B. J. Kooi, J. Th. M. De Hosson, and B. Noheda, J. Phys.: Condens. Matter **21**, 182001 (2009).
[17]X. Marti, V. Skumryev, V. Laukhin, R. Bachelet, C. Ferrater, M. V. García-Cuenca, M. Varela, F. Sánchez, and J. Fontcuberta, "Strain-driven noncollinear magnetic ordering in orthorhombic epitaxial $YMnO_3$ thin films" (unpublished).
[18]M. N. Iliev, M. V. Abrashev, H.-G. Lee, V. N. Popov, Y. Y. Sun, C. Thomsen, R. L. Meng, and C. W. Chu, Phys. Rev. B **57**, 2872 (1998).
[19]X. Marti, F. Sánchez, V. Skumryev, C. Ferrater, M. V. García-Cuenca, M. Varela, and J. Fontcuberta, Thin Solid Films **516**, 4899 (2008).
[20]B. Martínez, J. Navarro, Ll Balcells, and J. Fontcuberta, J. Phys.: Condens. Matter **12**, 10515 (2000).
[21]N. O. Moreno, J. G. S. Duque, P. G. Pagliuso, C. Rettori, R. R. Urbano, and T. Kimura, J. Magn. Magn. Mater. **310**, e364 (2007).
[22]V. Skumryev, M. Kuzmin, M. Gospodinov, and J. Fontcuberta, Phys. Rev. B **79**, 212414 (2009).
[23]X. Marti, I. Fina, V. Skumryev, C. Ferrater, M. Varela, L. Fábrega, F. Sánchez, and J. Fontcuberta, Appl. Phys. Lett. **95**, 142903 (2009).